Defects in hydrogenated amorphous silicon-carbon alloy films prepared by glow discharge decomposition and sputtering

Journal of Applied Physics

Defects in hydrogenated amorphous silicon-carbon alloy films prepared by glow discharge decomposition and sputtering

Cite as: Journal of Applied Physics **53**, 7299 (1982); https://doi.org/10.1063/1.329879
Submitted: 07 May 1982 • Accepted: 01 July 1982 • Published Online: 14 August 1998

A. Morimoto, T. Miura, M. Kumeda, et al.

Defects in hydrogenated amorphous silicon-carbon alloy films prepared by glow discharge decomposition and sputtering

A. Morimoto, T. Miura, M. Kumeda, and T. Shimizu
Department of Electronics, Faculty of Technology, Kanazawa University, Kanazawa 920, Japan

(Received 7 May 1982; accepted for publication 1 July 1982)

Properties of hydrogenated amorphous silicon-carbon alloy (a-$Si_{1-x}C_x$:H) films prepared by radio frequency (rf) glow discharge decomposition and rf sputtering have been investigated by means of electron spin resonance (ESR), infrared absorption, optical absorption, and photoconductivity measurements. Although the number of C-H per C atom [C-H]/[C] is larger than that of Si-H per Si atom [Si-H]/[Si], the ESR spin density increases greatly with the C content. The increase in the density of dangling bonds may be related to the fact that the number of H atoms in gathered phase increases with an increase in x. ESR measurements also give useful information about the preferential formation of C or Si dangling bonds and the atomic distribution of Si and C through a compositional dependence of the g value. A remarkable feature for a-$Si_{1-x}C_x$:H film is that the presence of C atoms in the amorphous network makes the Si-H bond in a-$Si_{1-x}C_x$:H more stable than that in a-Si:H.

PACS numbers: 61.16.Hn, 72.40. + w, 78.20.Dj, 61.40. − a

INTRODUCTION

During the past one or two years hydrogenated amorphous silicon-carbon alloy (a-$Si_{1-x}C_x$:H) films have attracted much attention because of the effectiveness of efficient solar cells[1] as well as the interesting alloy system for the study of amorphous materials.[2–7] The nature of defects and their relation to H atoms appear to be the most important problems in the investigation of a-$Si_{1-x}C_x$:H. However, there has been so far no electron spin resonance (ESR) study correlated with infrared (IR) absorption results except for a preliminary result for a-$Si_{1-x}C_x$:H prepared by radio frequency (rf) sputtering by the present authors.[8]

On the basis of the investigation of hydrogenated amorphous silicon-carbon alloy prepared by reactive rf sputtering (SP a-$Si_{1-x}C_x$:H)[8] and hydrogenated amorphous silicon-germanium alloy prepared by rf glow discharge decomposition (GD a-$Si_{1-x}Ge_x$:H),[9,10] we have found the following relation for the number of bonded hydrogen per atom:

$$\frac{[\text{C-H}]}{[\text{C}]} > \frac{[\text{Si-H}]}{[\text{Si}]} > \frac{[\text{Ge-H}]}{[\text{Ge}]}. \tag{1}$$

As pointed out by Paul *et al.*[9] [Ge-H]/[Ge] < [Si-H]/[Si] is mainly responsible for the fact that a-$Si_{1-x}Ge_x$:H film is more defective than a-Si:H. Therefore, the question arises; "Is the same discussion applied to a-$Si_{1-x}C_x$:H?" We have prepared a-$Si_{1-x}C_x$:H films by using rf sputtering and rf glow discharge decomposition methods, and measured ESR due to defects, IR absorption due to Si-H and C-H vibrations, photoconductivity, and optical absorption for these samples. In order to investigate an influence of the ordering of Si and C atoms and the bonding scheme of H, the SP films are prepared with various compositions and substrate temperatures, and GD films are prepared with various compositions, substrate temperatures, and flow rates of H_2 introduced into the deposition chamber. Furthermore, annealing of these films is carried out in order to investigate the change of the film properties by annealing. A preliminary result of the compositional dependence of the film properties for GD a-$Si_{1-x}C_x$:H was already reported.[11]

EXPERIMENTAL

The samples studied in this work were prepared both by rf glow discharge (GD) method and rf sputtering (SP) method. The GD samples were prepared by rf glow discharge decomposition of SiH_4 and CH_4 in a diode system with various rf powers, substrate temperatures, and flow rate ratios $r_Q = Q(CH_4)/[Q(SiH_4) + Q(CH_4)]$, where Q represents the flow rate. The diode was composed of 90 mmϕ cathode electrode and 200 mmϕ anode electrode, and electrodes spacing was 27 mm. Various substrates for various measurements were placed in the area of 100 mmϕ on the anode electrode. The various deposition parameters were summarized in Table I. In order to investigate the dependence of film properties on flow rate ratio r_Q, substrate temperature T_s and H_2 flow rate Q, the other deposition parameters were fixed as shown in the column of standard condition. The film thickness was 1–11 μm.

The SP samples were prepared by diode-type reactive rf sputtering. Composite target composed of crystalline Si (c-Si) chips and a graphite plate were sputtered in Ar-H_2 gas mixture of 3.9–4.9 Pa (3–3.5 $\times 10^{-2}$ Torr) with H_2 partial pressure ratio $r_P = P(H_2)/[P(H_2) + P(\text{Ar})]$ fixed at 40%. Applied rf power P_i was 200 W and substrate temperature T_s was varied from water-cooled temperature to 300 °C.

The films were deposited on 150-μm thick glass substrates for electrical and optical measurements, 500-μm-thick c-Si substrates with high resistivity (σ = 800–1000 $\Omega^{-1}\,\text{cm}^{-1}$) for IR absorption measurements, and aluminum foil substrates for ESR measurements. The aluminum foil substrates were dissolved in HCl solution before ESR measurements. Influence of Al foil substrate and soak in HCl solution were negligibly small, because there was no difference between the ESR signal for a certain film deposited on fused quartz substrate and that for the film deposited on Al

 0021-8979/82/117299-07$02.40

TABLE I. Deposition condition for GD a-$Si_{1-x}C_x$:H film.

	Used range	Standard condition
substrate temperature T_s (°C)	R.T.–400	350
rf power P_i (W)	20–100	100
SiH_4-CH_4 total flow rate Q (SCCM)	24	24
flow rate ratio $r_Q = \frac{Q(CH_4)}{Q(SiH_4)+Q(CH_4)}$	0–0.95	0.59
H_2 flow rate Q (SCCM)	0–200	0

foil. ESR, IR absorption, photoconductivity, and optical absorption measurements were carried out. The film composition was determined by electron probe microanalysis (EPMA).

Annealing of GD films was carried out in a vacuum of 8×10^{-5} Pa (6×10^{-7} Torr) for an hour.

RESULTS AND DISCUSSION

Figure 1 shows $(\alpha\hbar\omega)^{1/2}$ vs photon energy $\hbar\omega$, where α is the optical absorption coefficient. The absorption edge tends to shift to higher photon energies and to broaden with an increase in the C content x. This result is roughly in agreement with the result of Sussmann *et al.*[6] The optical gap E_g is obtained by fitting the absorption data to the expression

$$(\alpha\hbar\omega)^{1/2} = \sqrt{B}\,(\hbar\omega - E_g). \quad (2)$$

The results of the fitting are shown by solid line in the figure. For the films with $x = 0$, there is only a small difference both in E_g and $\sqrt{B}$ between the 20-W film and 100-W film. However, the differences in $\sqrt{B}$ and E_g tend to increase as x is increased; a decrease in rf power appears to lead to an increase in $\sqrt{B}$ and a slight increase in E_g.

Figure 2 shows the spin density N_s derived from the ESR signal as a function of the C content x for films prepared by GD and SP methods. The ESR signals are considered to originate from dangling bonds of Si or C atoms. The spin density N_s for GD films significantly increases by about 4 orders of magnitude as x is increased from 0–0.77. Although N_s for SP films also shows a similar x dependence, N_s for SP films is larger than that for GD films by more than one order of magnitude.

Corresponding to the behavior of N_s for GD films, photoconductivity σ_p and $\eta\mu\tau$ also significantly decrease by about 4 orders of magnitude as x is increased from 0 to 0.3, regardless of the rf power, where η is the quantum efficiency, μ is the drift mobility, and τ is the carrier lifetime. The $\eta\mu\tau$ is measured at the photon energies of 1.96 eV (He-Ne laser $\lambda = 6328$ A) and 2.41 eV (Ar laser $\lambda = 5145$ A). The $\eta\mu\tau$ observed at 1.96 eV is larger than that at 2.41 eV by more than one order of magnitude for all the compositions. Since the quantum efficiency η at 1.96 eV is not considered to differ from that at 2.41 eV by more than one order, the more

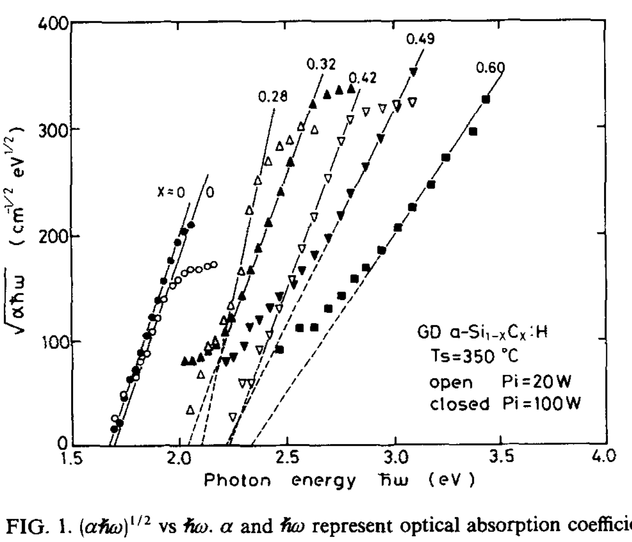

FIG. 1. $(\alpha\hbar\omega)^{1/2}$ vs $\hbar\omega$. α and $\hbar\omega$ represent optical absorption coefficient and photon energy, respectively.

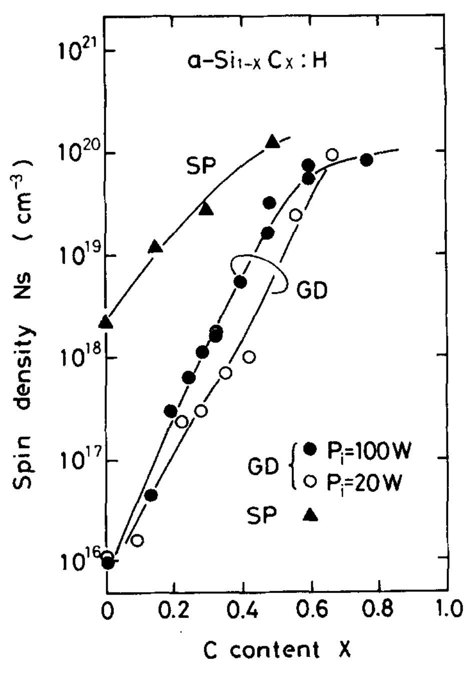

FIG. 2. Spin density N_s for GD and SP a-$Si_{1-x}C_x$:H films as a function of x. GD films are prepared at $T_s = 350$ °C, and SP films are prepared at $T_s = 300$ °C.

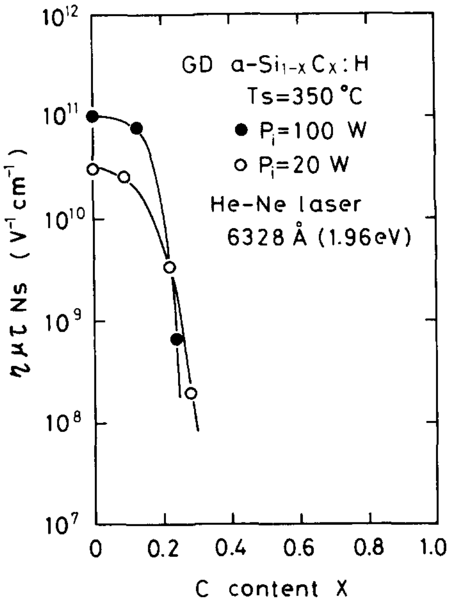

FIG. 3. $\eta\mu\tau N_s$ for GD films as a function of C content x.

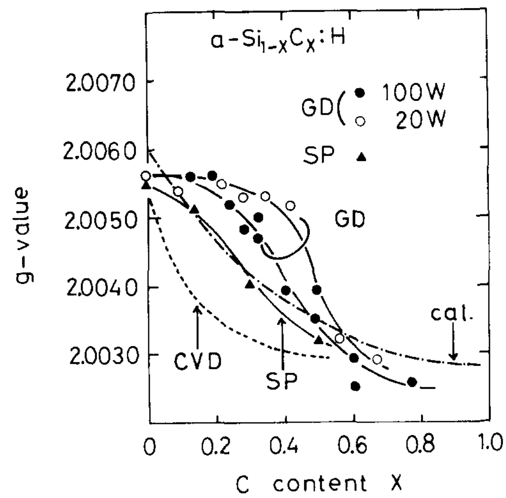

FIG. 4. g value of ESR signal for GD and SP a-$Si_{1-x}C_x$:H films as a function of x. GD films are prepared at $T_s = 350$ °C, and SP films are prepared at $T_s = 300$ °C. Results of CVD films are also shown by dashed curve for comparison. Dotted-and-dashed curve represents result obtained by calculation by using simple molecular orbital methods.

defective surface layer that absorbs most of the photons with the energy of 2.41 eV may be responsible for the smaller value of $\eta\mu\tau$. Therefore, we discuss only the $\eta\mu\tau$ observed at 1.96 eV. Since the thickness of the film used for the photoconductivity measurement ranges from 2 to 4 μm, the surface effect is expected not to be important for the photoconductivity with photon energy of 1.96 eV. In order to investigate origins of the significant decrease of $\eta\mu\tau$ described above, $\eta\mu\tau N_s$ is plotted against x in Fig. 3. If it is assumed that the recombination center for photoexcited carriers is mainly the dangling bond and the carrier lifetime τ is proportional to the reciprocal dangling bond density $1/N_s$, then $\eta\mu\tau N_s$ is proportional to μ, where η is assumed to be constant. In the figure $\eta\mu\tau N_s$ is decreased by 2 orders of magnitude as x is increased from 0 to about 0.3. Therefore, it is suggested that the decrease in μ as well as the increase of N_s with an increase in x is responsible for the significant decrease in $\eta\mu\tau$.

Although the spin density of the ESR signal due to Si dangling bonds and that due to Ge dangling bonds can be separated for GD a-$Si_{1-x}Ge_x$:H films,[8,10] those due to Si and C dangling bonds cannot be separated for GD a-$Si_{1-x}C_x$:H films. The reason is as follows: though there is a large difference both in g value and linewidth between the ESR signal due to Si dangling bonds and that due to Ge dangling bonds, there is only a small difference in g value and linewidth between the ESR signal due to Si dangling bonds and that due to C dangling bonds. Since we cannot separate the observed ESR signal into those due to the two kinds of dangling bonds, we investigated the change in the g value related to the ease of the formation of Si or C dangling bonds.

Figure 4 shows the g value of the ESR signal as a function of the C content x. The g value for GD films deposited at rf power of 100 W decreases gradually in the Si-rich composition range ($x < 0.2$), and reaches the g value of the C dangling bond, 2.003, rather abruptly around $x = 0.5$. The g value for films prepared at 20 W appears to decrease more gradually than that for films deposited at 100 W. This behavior is different from the results of SP and CVD films. The g value of SP films decreases more rapidly than that of GD films as x increases. In this figure, the results for a-$Si_{1-x}C_x$:H films prepared by CVD[12] are also shown by the dashed curve for comparison. The g value for CVD films decreases most abruptly from 2.0055 to 2.003 by the incorporation of a small amount of C in the g values of films prepared by various deposition methods. These various compositional dependences of the g value suggest that the various deposition methods lead to various ratios of the number of C dangling bonds per C atom [C↑]/[C] to that of Si dangling bonds per Si atom [Si↑]/[Si] and/or various atomic distributions.

To discuss this in more detail, we consider three different atomic distributions: random distribution, phase separation, and chemical ordering. The dotted-and-dashed curve included in Fig. 4 for comparison is obtained by a calculation based on a simple molecular orbital method.[13] The calculation is carried out by assuming that Si and C atoms are randomly distributed and [C↑]/[C] = [Si↑]/[Si]. The reason why the calculated result displays downward curvature is that the g value of Si dangling bonds with nearest-neighbor C atoms is smaller than that without nearest-neighbor C atoms.[13] If Si and C atoms are phase separated, there are few chances for Si dangling bonds to have nearest-neighbor C atoms and the dependence of g value on x should be linear when [C↑]/[C] = [Si↑]/[Si]. In the case of chemical ordering, the g value of Si dangling bonds is expected to be much smaller than that in the case of random distribution because the Si dangling bonds are more likely to have nearest-neighbor C atoms.

The observed g value for GD films in the range of small x appears to be larger than the linear compositional dependence expected in the case of phase separation. We can, therefore, conclude that in the Si-rich composition range

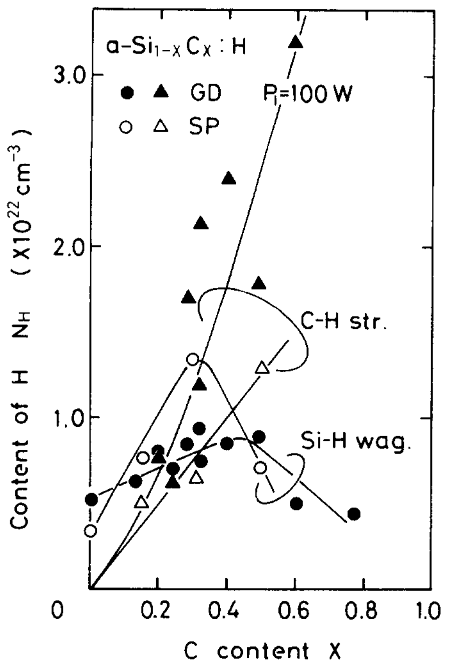

FIG. 5. Contents of H atoms bonded to Si and C atoms for GD and SP films N_H as a function C content x. GD films and SP films are prepared at T_s = 350° and 300 °C, respectively.

($x<0.3$), [Si↑]/[Si] is larger than [C↑]/[C], regardless of the atomic distribution. The fact that the g value for CVD films is much smaller than those for GD and SP films indicates that ([C↑]/[C])/([Si↑]/[Si]) for CVD films is larger than that for the others and/or Si and C atoms for CVD films tend to be more chemically ordered than those for the others. It is reasonable that CVD films have a tendency of the chemical ordering in comparison with GD and SP films because the substrate temperature T_s for CVD films is 630 °C which is higher than 350° and 300 °C, for GD films and SP films, respectively. The higher T_s is considered to lead to more stable chemical ordering than phase separation.

Figure 5 shows the content of H atoms bonded to Si and C atoms N_H for GD and SP films as a function of the C content x. N_H is estimated from the intensity of the IR absorption due to the Si-H wagging mode (630 cm^{-1}) and the C-H stretching mode (3000 cm^{-1}) absorption. We used the C-H stretching mode absorption because the C-H wagging, rocking, bending mode, and the like are distributed over the wide wave number range of 900–1500 cm^{-1} depending on various vibrational modes and various environments of the C atoms and it is difficult to identify each mode. Although Wieder *et al.*[7] reported that the absorption at 780 cm^{-1} is due to Si-CH_3 vibration, we suggest that the absorption at 780 cm^{-1} is not related to H but is due to the Si-C transverse optical mode because this absorption with a similar intensity is observed for a-$Si_{1-x}C_x$:H with and without H.

In order to estimate the H content from the intensity of IR absorptions, we took $A = 1.6\times10^{19}$ cm^{-2} [14] and $A = 1.7\times10^{21}$ cm^{-2} for Si-H wagging mode and C-H stretching mode, respectively, where A is defined by the following equation:

$$N_H = A \times \int (\alpha/\omega)\, d\omega. \tag{3}$$

Here, α is the absorption coefficient and ω is the wave number. The oscillator strength of the C-H stretching mode is determined by comparing the results of the IR absorption with those of nuclear magnetic resonance (NMR) of H in GD a-$Si_{1-x}C_x$:H films.[15] NMR measurements were carried out for the present a-$Si_{1-x}C_x$:H films with $0<x<0.77$ and a-C:H films prepared under a different deposition condition, and the oscillator strength was found to be roughly constant for these films.

We can also estimate the content of H atoms bonded to the Si atom [Si-H] from the Si-H stretching mode, and it is confirmed that the compositional dependence derived from Si-H stretching mode in GD and SP films qualitatively agrees with that derived from the Si-H wagging mode. In spite of the decrease in the Si content, [Si-H] for GD and SP film is found to increase with an increase in the C content x in Si-rich composition range. Detailed discussions on this point will be described later. Here, we define the preferential attachment of H atom to C atom as follows[9]:

$$P = \frac{[\text{C-H}]/[\text{C}]}{[\text{Si-H}]/[\text{Si}]}. \tag{4}$$

Evaluating this factor from the figure, we obtain $P = 2.1$–5.1 for GD film and $P = 1.1$–3.6 for SP films. In both films, [C-H]/[C] is larger than [Si-H]/[Si] and N_s largely increases with an increase in x. It should be noted that the density of defects increases with an increase in x in spite of an increase in the H content. The result suggests that the density of defects in a-$Si_{1-x}C_x$:H is governed not only by the content of H atoms bonded to Si and C atoms but also the incorporation scheme of H and the matrix structure. Although the origin of the increase in N_s is not so clear, the following may be responsible for it. (1) The bond length for C-C, 1.54 Å, is far smaller than that for Si-Si, 2.35 Å. (2) The coordination number of C atoms tends to be three. (3) Most of the H atoms are in the gathered phase as shown below.

In order to get information on the incorporation scheme of H we investigate the shape of the Si-H stretching mode absorption. Figure 6 shows the compositional dependence of the absorption line shape of Si-H stretching mode for GD and SP films. There appears to be no essential difference between the films prepared with the different rf powers. In both Figs. 6(a) and 6(b), it is very clear that the absorption bands for the film with $x=0$ peak mainly at 2000 cm^{-1} and those for films with $x>0.2$ peak mainly at 2090 cm^{-1}. An increase in x leads to a disappearance of the shoulder around 2000 cm^{-1} and an appearance of the shoulder around 2090 cm^{-1}. In a-$Si_{1-x}C_x$:H films the absorption at 2000 cm^{-1} could be the Si-H stretching mode of SiH without nearest-neighbor C atoms and the absorption at 2090 cm^{-1} could be attributed either to Si-H stretching mode of SiH_2 or to the shift of the SiH stretching mode due to the presence of nearest-neighbor C atoms. Wieder *et al.*[7] attributed the shift of the 2000 cm^{-1} peak to a higher wave number with an increase in x mainly to C atoms at the site neighboring the SiH in order to keep the number of parameters in their model under control, though the weak absorption around 900

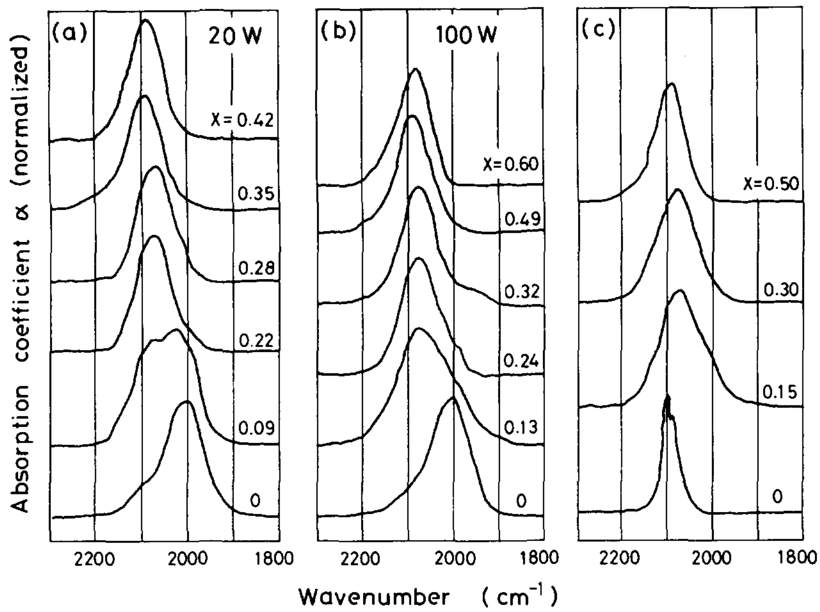

FIG. 6. Compositional dependence of absorption line shape of Si-H stretching mode for GD and SP films. Absorption intensities are normalized: (a) for 20-W GD films, (b) for 100-W GD films, and (c) for SP films. Narrowing of line shape for SP films with $x = 0$ is attributed to crystallization of film.

cm^{-1} due to SiH_2 bending mode was observed. In the present case we suggest the content of SiH_2 cannot be negligible because of two bits of evidence. First, there is a weak SiH_2 bending band at about 900 cm^{-1} even for the film with $x = 0$, and the absorption intensity appears to be gradually increased with an increase in x, though it is difficult to be distinguished from the large absorptions near 1000 cm^{-1} band and 780 cm^{-1} band for the films with $x > 0.3$. Second, the compositional dependence of the absorption line shape for GD films [Figs. 6(a) and 6(b)] with $x > 0.2$ well resembles that for SP films [Fig. 6(c)] with $x > 0$ which is considered to have H atoms of SiH_2 type because of the significant bending mode absorption; that is, the peak of Si-H stretching mode is approximately fixed at 2090 cm^{-1} and only the center of gravity moves to a higher wave number. Thus, the formation of SiH_2 as well as the shift of SiH stretching mode due to the presence of nearest-neighbor C atoms can be regarded as a main origin of the 2090 cm^{-1} band. A rapid increase in [Si↑]/[Si] for Si-rich GD films described above might partly be attributed to the formation of SiH_2 with the small C incorporation, as is often observed for a-Si:H films. In a similar way, the formation of dispersed CH_2,CH_3 and the like is considered to be responsible for the significant increase of N_s for GD films over all the composition. Such information can be obtained by ^{1}H NMR measurements. The results of NMR in GD a-$Si_{1-x}C_x$:H films[15] suggest that the number of H atoms in gathered phase increases greatly and the number of H atoms in dispersed phase hardly increases with an increase in the C content x. H atoms in dispersed phase is considered to play a role of reducing the density of dangling bonds, but those in gathered phase have nothing to do with decreasing dangling bonds.[16]

As seen from Fig. 6(c) the film with $x = 0$ has a sharp absorption line shape, though those with $x > 0$ have a broad absorption line shape. We confirmed by both x-ray diffraction and Raman scattering that the film with $x = 0$ is crystallized while those with $x > 0$ are amorphous. Therefore, the sharpness of the line shape is considered to be due to the crystallization of the film.[17] This result suggests that the C atom in a-$Si_{1-x}C_x$:H film works as a glass former.

In order to discuss the origin of the formation of the defects accompanied by the C incorporation into the film in detail, we investigate dependences of N_s on T_s, annealing temperature T_a and flow rate of H_2 during the glow discharge deposition. Figure 7 shows the spin density N_s for the GD and SP films as a function of T_s. The result of EPMA

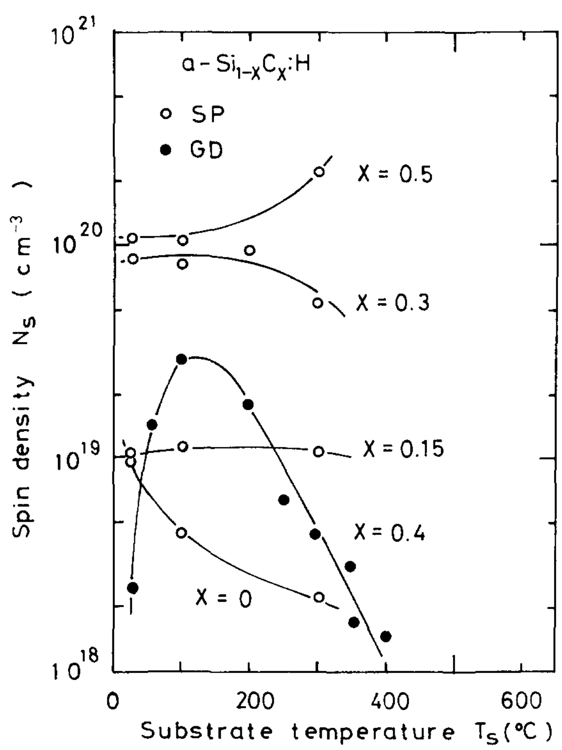

FIG. 7. Spin density N_s for GD and SP films as a function of substrate temperature T_s. GD and SP films are prepared with a fixed flow rate ratio $r_Q = 0.59$ and fixed area ratios of c-Si chips to graphite plate, respectively.

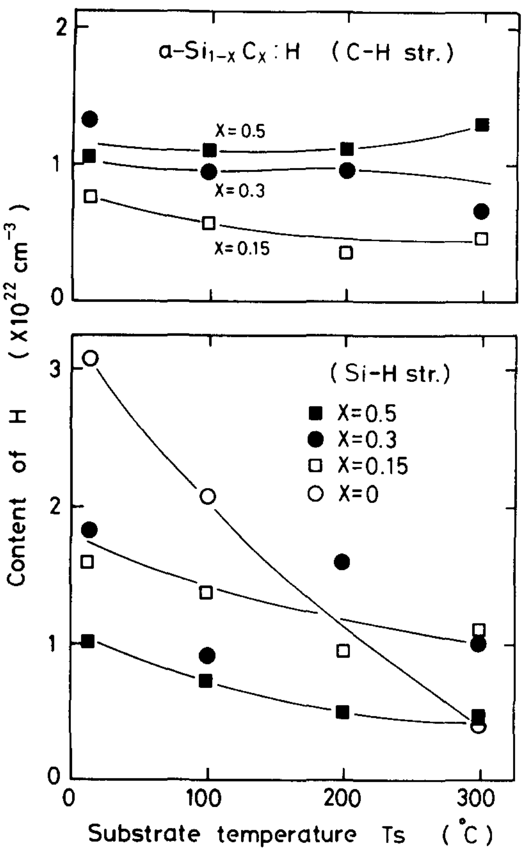

FIG. 8. Content of H, N_H, for SP films with various compositions as a function of substrate temperature T_s.

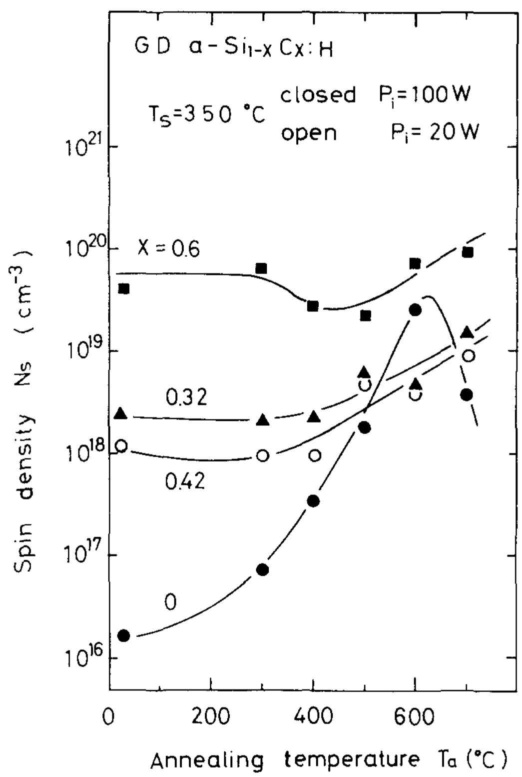

FIG. 9. Spin density N_s for GD films with various compositions as a function of annealing temperature T_a.

measurement shows that the C content x of GD and SP film are roughly constant for fixed flow rate ratio and area ratio, respectively. As seen in Fig. 7, the change in N_s with T_s for GD films differs from that for SP films. N_s for GD films depends upon T_s. On the other hand N_s for SP films with $x>0$ is roughly independent of T_s, though N_s for SP films with $x=0$ depends on T_s. The increase in N_s for GD films around $T_s = 100$ °C appears to be attributed to the increase in the Si dangling bonds, because the corresponding g value also has a small maximum at about $T_s = 100$ °C. The reason why there is such a dependence of N_s on T_s for GD a-$Si_{1-x}C_x$:H films is not clear, because there is no marked change in N_H for these films.

Figure 8 shows the dependence of the content of H, for SP films on substrate temperature T_s. [C-H] is almost independent of T_s, regardless of the film composition. [Si-H] for SP a-$Si_{1-x}C_x$:H does not largely decrease with an increase in T_s, while [Si-H] for SP a-Si:H significantly decreases with an increase in T_s. These findings indicate that the C incorporation makes the film structure more heat resistant.

Figure 9 shows the spin density N_s for GD films with various compositions as a function of annealing temperature T_a. N_s for the films with $x=0$ rapidly increases from 10^{16} to 10^{19} cm^{-3} as T_a increases up to 600 °C and decreases by one order of magnitude as T_a reaches 700 °C. This decrease of N_s may be mainly attributed to crystallization of a-Si:H film. On the contrary N_s's for the films with $x=0.32$ and 0.42 increase at most only by one order of magnitude as x increases from 400° to 700 °C, regardless of the rf power. The g value for the corresponding films decreases from 2.0050 to 2.0042 as T_a increases from 400° to 700 °C. As it is unlikely that [C↑]/[C] increases more rapidly than [Si↑]/[Si] because C-H bonds are more heat resistant than Si-H bonds, the annealing up to 700 °C probably leads to rearrangement of Si and C atoms after the evolution of H atoms and to the chemical ordering of Si and C atoms. Comparing the results of the films with $x=0$ and $x=0.32$–0.42, we find that GD a-$Si_{1-x}C_x$:H film is remarkably more heat resistant than a-Si:H films as in the case of SP a-$Si_{1-x}C_x$:H films.[8] N_H for the film with $x=0.6$ is measured at various T_a's. A prominent evolution of H atoms from Si and C atoms is observed at about $T_a = 600$ °C, as observed for SP a-$Si_{1-x}C_x$:H films in our previous study.[8] Comparing this result with the fact that H atoms in a-Si:H are markedly evolved at about $T_a = 400$ °C, we find that the presence of C atoms in the amorphous network can prevent H atoms bonded to the Si atom from being effused out. In other words, a-$Si_{1-x}C_x$:H films are more heat resistant than a-Si:H films.

The striking characteristic of a-$Si_{1-x}C_x$:H is the heat resistance, regardless of the preparation method. On the basis of the results of thermal property measurement, for example, the dependence of N_H for SP a-$Si_{1-x}C_x$:H films on T_s, the dependence of N_H for GD a-$Si_{1-x}C_x$:H films on T_a, and so on, we find that the Si-H bonds in a-$Si_{1-x}C_x$:H films become more stable against heating than those in a-Si:H. Therefore, it is reasonable that as shown in Fig. 5 [Si-H] increases with an increase in the C content x in the Si-rich composition range. In short, the C atom in a-$Si_{1-x}C_x$:H can

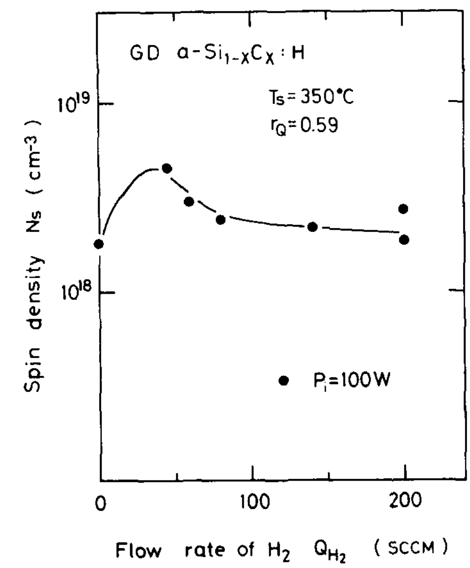

FIG. 10. Spin density N_s for GD films with $r_Q = 0.59$ as a function of flow rate of H_2, $Q(H_2)$.

act as a stabilizer of the Si-H bond. This property appears to result in the fact that the dependence of N_s on T_s and T_a for a-$Si_{1-x}C_x$:H is weak. This function of C atoms as well as the glass former may be very important in a device application of the film.

Figure 10 shows the spin density N_s for GD films as a function of the flow rate of H_2, $Q(H_2)$. The other deposition parameters are standard as shown in Table I. The dependence of N_s on $Q(H_2)$ has a maximum around $Q(H_2) = 50$ SCCM. The C content x determined by EPMA also has a maximum value around $Q(H_2) = 50$ SCCM; x increases from 0.32 to 0.42 and then decreases to 0.26, as $Q(H_2)$ increases from 0 to 200 SCCM. This content shift toward a C-rich composition is consistent with the observed changes of the $(\alpha\hbar\omega)^{1/2}$ vs $\hbar\omega$ relation, [C-H] and [Si-H], and g value. Therefore, we conclude that an incorporation of H_2 gas into glow discharge deposition chamber leads to only the content deviation toward a C-rich composition and has no direct influence on film property.

CONCLUSION

(1) Although the number of C-H per C atom [C-H]/[C] is larger than that of Si-H per Si atom [Si-H]/[Si], the spin density N_s for the GD films significantly increases from 10^{16} to 10^{20} cm^{-3} as the C content x increases from 0 to 0.77.

(2) It is suggested that the increase in the C content leads not only to the reduction of the carrier lifetime τ through the increase in N_s but also to the reduction of the drift mobility μ on the basis of assumption of $\tau \propto 1/N_s$.

(3) The compositional dependence of the g value of the ESR signal for a-$Si_{1-x}C_x$:H films changes considerably with preparation methods. The compositional dependence gives us useful information about the ease of the formation of C dangling bonds compared with that of Si dangling bonds and the atomic distribution.

(4) Possible origins of the significant increase in N_s for GD films with C incorporation are summarized as follows: (i) The change of the incorporation scheme of H atoms, i.e., from the H atoms in the dispersed phase to the H atoms in the gathered phase. (ii) The difference of the bond length between Si-Si and C-C. (iii) The tendency for the coordination number of C atoms to be three.

(5) The presence of C atoms in the amorphous network makes the Si-H bond more stable in a-$Si_{1-x}C_x$:H than that in a-Si:H. The fact makes a-$Si_{1-x}C_x$:H films more heat resistant than a-Si:H films.

ACKNOWLEDGMENTS

We would like to thank K. Tanahashi, T. Nishikawa, N. Matsumoto, and K. Yoshida for their technical assistance. This work was partly supported by the Sunshine Project of the Ministry of International Trade and Industry in Japan.

[1] Y. Tawada, H. Okamoto, and Y. Hamakawa, Appl. Phys. Lett. **39**, 237 (1981).
[2] D. A. Anderson and W. E. Spear, Philos. Mag. **35**, 1 (1977).
[3] Y. Catherine and G. Turban, Thin Solid Films **60**, 193 (1979).
[4] H. Munekata, S. Murasato, and H. Kukimoto, Appl. Phys. Lett. **37**, 536 (1980).
[5] Y. Katayama, K. Usami, and T. Shimada, Philos. Mag. B **43**, 283 (1981).
[6] R. S. Sussmann and R. Ogden, Philos. Mag. B **44**, 137 (1981).
[7] H. Wieder, M. Cardona, and C. R. Guarnieri, Phys. Status Solidi B **92**, 99 (1979).
[8] T. Shimizu, M. Kumeda, and Y. Kiriyama, *Tetrahedrally Bonded Amorphous Semiconductors*, Carefree, Arizona, 1981 (AIP Conf. Proc. No. 73, AIP New York, 1981) p. 171.
[9] W. Paul, D. K. Paul, B. von Roedern, J. Blake, and S. Oguz, Phys. Rev. Lett. **46**, 1016 (1981).
[10] A. Morimoto, T. Miura, M. Kumeda, and T. Shimizu, Jpn. J. Appl. Phys. **20**, L833 (1981).
[11] A. Morimoto, T. Miura, M. Kumeda, and T. Shimizu, Jpn. J. Appl. Phys. **21**, L119 (1982).
[12] P. H. Gaczi and D. C. Booth, Sol. Energy Mater. **4**, 297 (1981).
[13] N. Ishii, M. Kumeda, and T. Shimizu, Solid State Commun. **41**, 143 (1982).
[14] H. Shanks, C. J. Fang, L. Ley, M. Cardona, F. J. Demond, and S. Kalbitzer, Phys. Status Solidi B **100**, 43 (1980).
[15] K. Nakazawa, S. Ueda, M. Kumeda, A. Morimoto, and T. Shimizu, Jpn. J. Appl. Phys. **21**, L176 (1982).
[16] T. Shimizu, K. Nakazawa, M. Kumeda, and S. Ueda, Jpn. J. Appl. Phys. **21**, No. 6 (1982).
[17] T. Imura, K. Mogi, A. Hiraki, S. Nakashima, and A. Mitsuishi, Solid State Commun. **40**, 161 (1981).